Pacific Northwest
NATIONAL LABORATORY

PNNL-36877

Advanced CO2 Capture Solvent Systems for Dynamic Power Generation

Quarterly Research Performance Progress Report: QR4 (Q4FY24)

November 2024

Zirui Mao
Zhijie Xu
Yuan Jiang

U.S. DEPARTMENT of ENERGY

Prepared for the U.S. Department of Energy
under Contract DE-AC05-76RL01830

DISCLAIMER

PACIFIC NORTHWEST NATIONAL LABORATORY
operated by
BATTELLE
for the
UNITED STATES DEPARTMENT OF ENERGY
under Contract DE-AC05-76RL01830

Printed in the United States of America

Available to DOE and DOE contractors from
the Office of Scientific and Technical Information,
P.O. Box 62, Oak Ridge, TN 37831-0062
www.osti.gov
ph: (865) 576-8401
fox: (865) 576-5728
email: reports@osti.gov

Available to the public from the National Technical Information Service
5301 Shawnee Rd., Alexandria, VA 22312
ph: (800) 553-NTIS (6847)
or (703) 605-6000
email: info@ntis.gov
Online ordering: http://www.ntis.gov

PNNL-36877

Advanced CO2 Capture Solvent Systems for Dynamic Power Generation

Quarterly Research Performance Progress Report: QR4 (Q4FY24)

November 2024

Zirui Mao
Zhijie Xu
Yuan Jiang

Prepared for
the U.S. Department of Energy
under Contract DE-AC05-76RL01830

Pacific Northwest National Laboratory
Richland, Washington 99354

Quarterly Research Performance Progress Report

QR4 (Q4FY24)

Advanced CO_2 Capture Solvent Systems for Dynamic Power Generation

Submitted to: U.S. Department of Energy / ARPA-E

DOE/ARPA-E Award #:	DE-AR0001717
Prime Recipient:	Research Triangle Institute Post Office Box 12194 Research Triangle Park, NC 27709-2194
DUNS Number:	004868105
Principal Investigator:	Dr. Paul Mobley Research Chemical Engineer pdmobley@rti.org (919) 541-6918
Project Partners:	Pacific Northwest National Laboratory (PNNL), Electric Power Research Institute (EPRI), Carbon Capture Simulation for Industrial Impact (CCSI^2), West Virginia University (WVU), SLB, and Mojonnier USA
Project Period:	September 19, 2023 – December 18, 2025
Reporting Period:	July 1, 2024 – September 30, 2024
Report Frequency:	Quarterly
Submission Date:	October 30, 2024

Signature of Submitting Official:

Acknowledgement

This material is based upon work supported by the Department of Energy under Award Number DE-AR0001717.

Disclaimer

Table of Contents

Abbreviations

ACM	Aspen Custom Modeler®
APD	Aspen Plus Dynamics®
CFD	Computational Fluid Dynamics
CO_2BOL	CO_2 Binding Organic Liquid
DCC	Direct Contact Cooler
ENRTL-SR	Electrolyte Non-Random Two Liquid Framework with Symmetric Reference
GT	Gas Turbine
HRSG	Heat Recovery Steam Generator
LCOE	Levelized Cost of Electricity
MEA	Monoethanolamine
NAS	Non-Aqueous Solvent
NCCC	National Carbon Capture Center
NGCC	Natural Gas Combined Cycle
NGCC-CCS	Natural Gas Combined Cycle with Carbon Capture and Storage
NPV	Net Present Value
OPEX	Operating Expense
PC	Pulverized Coal
PFD	Process Flow Diagram
PVT	Pressure-Volume-Temperature
RK	Redlich-Kwong
ROM	Reduced Order Model
RPB	Rotating Packed Bed
SDoE	Sequential Design of Experiments
SRD	Specific Reboiler Duty
ST	Steam Turbine
TCR	Total Capital Requirement
TEG	Triethylene Glycol
TPC	Total Plant Cost
WLS	Water-Lean Solvent
VLE	Vapor-Liquid Equilibrium

Project Overview

Phase 1 Background. Phase 1 focused on developing dynamic models to represent and optimize a variable NGCC-CCS process and experimental work to reduce the uncertainty and improve prediction accuracy in the dynamic model predictions. The modeling work included adapting existing steady-state CO_2 capture and dynamic NGCC and CO_2 compression models and adding new components, such as RPBs, to dynamic models or refining existing dynamic models for more rigorous integration. A dispatch model was developed to support the NPV optimization. Measurement of lab-scale properties of each solvent were performed for NG flue gas conditions to extend existing coal-based models. Bench-scale testing was completed at RTI with conventional and process intensified configurations to gain data for dynamic model validation. CFD modeling with the specific RPB geometry tested at RTI was completed and correlations for pressure drop, solvent holdup, and interfacial area were developed to be integrated in the RPB model.

The NAS and EEMPA models were evaluated in the dispatch model at different CO_2 capture rates to determine the operating range to focus on for NPV optimization. The final cost estimation was completed with laying out the cost assumptions and a process flow diagram to represent the proposed system. The framework of the NPV optimization tool was completed and was set up to simultaneously optimize the process design and operation depending on the electricity and carbon prices.

Phase 2 Objectives. The objectives in Phase 2 will be de-risking the scale-up and operation of rotating packed bed (RPB). By the end of the project we will i) build and conduct factory acceptance and mass transfer testing of demonstration-scale RPB unit with capacity for capturing 100 t-CO_2/day; ii) develop control strategies for RPB unit integration with existing NGCC-CCS plants; iii) demonstrate ability for RPB to reduce DCC and absorber size 10X compared to conventional columns; iv) design and estimate costs for 100 t-CO_2/day RPB demonstration system v) identify host site for field demonstration of this RPB demo system; vi) identify system integrator(s) for RPB demonstration system, vii) develop conceptual design and identify commercialization partner for RPB based NGCC-CCS system with >1000 t-CO_2/day capacity; and viii) demonstrate bare erected cost (BEC) targets below \$638/(t-CO_2/day) and \$508/(t-CO_2/day) for commercial-scale RPB used as an absorber and DCC, respectively.

Phase 2 Approach. The project team has the following approach to address the Phase 2 objectives:
Performance Risks in Scale-up and Operation of RPB. In Phase 1, bench-scale testing confirmed high CO_2 capture rate in an RPB can be achieved and thus used as a CO_2 absorber. Large capital expense reductions can be gained using an RPB as a direct contact cooler (DCC) and water washes in the capture process. The suitability for RPB to be used as DCC and water wash will be evaluated at the bench scale (Task 3.1). The design of demonstration-scale RPB will be based on the results gathered from bench-scale testing, CFD simulation, and current manufacturing limitations (Task 3.1/3.2/3.4) and in line with commercial scale conceptual design (Task 3.3). The fabrication and performance testing of RPB will address mechanical challenges associated with the demonstration-scale build (Task 4.2-4.4).

CAPEX and Cost Estimation Risks. The uncertainty of RPB fabrication cost estimate of RPB will be greatly reduced as the capacity of the demonstration-scale RPB fabricated in this project will be within an order of magnitude of the projected commercial RPB unit. The hardware costs for the DCC, absorber, and washes will be updated with improved accuracy RPB CAPEX estimate and an updated conceptual design and BEC for a commercial scale RPB absorber and DCC (Task 4.5/5.3).

NGCC-CCS System Integration Risks. Detailed analysis of the operation of RPBs for scale-up to an NGCC power plant are needed to address commercialization risks (Task 4.3, 4.4). System integration analyses are also required i) to determine control strategies for integrated systems under different scenarios (Task 2.2,

4.7), ii) for risk identification and mitigation for permitting (Task 5.4) and CO_2 transportation and storage (T&S, Task 2.3), and iii) updating the overall NGCC-CCS integrated system retrofit and OPEX costs (Task 2.4, 4.5).

Demonstration System Planning. A host site with NGCC-relevant flue gas available at ~100 t-CO_2/day (Task 5.1) will be identified. A process FEED package will be developed and a cost estimate for the demonstration scale testing (Task 5.2). A constructability review will bed completed for the demonstration system and commercial RPB design (Task 5.4).

Executive Summary

Progress is reported for the period from June 1, 2024 to September 30, 2024. This quarterly report concentrates on a summary of work performed under Tasks 2, 3, 5, and 6. The project is progressing well with the previous team members as well as two new project partners. The team has met regularly in separate task-oriented meetings and the team is aligned with the project goals and approach. An overview of the current status of the project objectives and milestones are as follows:

Task 2: NGCC-CCS System Integration Risks.

- The project team met in Q1 to outline the modeling approach with the goal to understand the capabilities of the technologies in dynamic operation. Focus will be paid to the dynamics of specific startup/shutdown/ramping scenarios of an integrated system.
- Dynamic modeling of a CO_2 capture system using EEMPA is still in development.
- An optimal control system approach is being evaluated to have the CO_2 capture system react to changes in flue gas flow rate proactively to minimize fluctuations.
- Dynamic modeling of CO_2 transportation and storage in an aquifer over the course of a year have been completed based on load profiles produced in Phase 1. Mitigation strategies to minimize impacts of intermittent CO_2 flow rates have been evaluated and costs will be estimated in the next quarter.

Task 2: CAPEX and Cost Estimation Risks.

- The CAPEX and cost estimation of the overall NGCC-CCS system and the commercial scale RPB are underway. EPRI began updating the equipment list and heat and material balance based on Phase 1 results. Mojonnier is also working to compile an equipment list for the 1000 t-CO_2/day unit based on the 100 t-CO_2/day unit design.

Task 3: Performance Risks in Scale-up and Operation of RPB.

- Milestones 1.1 and 3.1 were completed on schedule and are detailed in the Q1 report, including a completed risk analysis of the commercial scale RPB conceptual design.
- The detailed design of a larger scale bench-scale RPB unit has been completed by Mojonnier in consultation with RTI. The fabrication of the unit is complete and was shipped to RTI following factory acceptance testing this quarter. The unit is being installed at RTI and testing will begin in the following quarter.
- A smaller unit was sent to RTI from Mojonnier in Q1 for initial testing of different packing geometries and porosities. Initial flooding tests indicated that the RPB capacity was larger than the existing infrastructure and modifications were made to expand the operating range that could be explored.
- Interfacial area measurements were collected from multiple different packing materials, porosities, and geometries to better understand the effects of each parameter on the effective area for mass transfer in the RPB. These tests will be expanded to the larger bench-scale unit in the next quarter to confirm scaling up principles.
- The liquid distribution in the CFD model was updated to the current nozzle design in use in the RPB. CFD capabilities to include heat transfer in the model were added to be able to simulate the temperature profile within the RPB packing.

- The detailed design of the 100 t-CO_2/day RPB is complete and an initial design review has been completed in the design team and with the fabricator. The cost estimate will be completed in the next quarter.
- A site visit to the fabrication shop will be completed in the next quarter to begin detailed discussions of the test setup.

Task 5: Demonstration System Planning.

- Discussions with multiple potential host sites have been started and will be continued in the coming quarter.
- Discussions with potential system integrators have also been conducted this quarter and will continue in the coming quarter.

Task 6: Tech to Market.

- An initial Tech to Market Plan was compiled in Q1 and has been updated each quarter since and submitted to DOE as a stand-alone document.

Progress on Pending Milestones

- Milestone 2.1: Dynamic modeling of the carbon capture system with a water-lean solvent is underway. The model development is progressing, and initial results are expected in the next quarter. The project team is still working with electricity production companies to attain representative NGCC plant data that can be used for NGCC model validation for startup and shutdown.
- Milestone 3.1: An RPB was integrated into the Bench-scale Gas Absorption System at RTI for performance evaluation of different packing options and different process unit applications. Testing has been completed to understand the impact of different packing characteristics on effective area. Testing has not been completed in the different unit operations as the team has not finalized which solvents to test in the absorber and wash sections with DOE. The system is set up and ready to test when the solvents are determined.

Progress on Future Milestones

- Milestone 2.4: The CAPEX and cost estimation of the overall NGCC-CCS system and the commercial scale RPB were both kicked off this quarter. EPRI began updating the equipment list and heat and material balance based on Phase 1 results. Mojonnier is also working to compile an equipment list for the 1000 t-CO_2/day unit based on the 100 t-CO_2/day unit design.
- Milestone 3.2: The liquid distribution in the CFD model was updated to the current nozzle design in use in the RPB. CFD capabilities to include heat transfer in the model were begun to be able to simulate the temperature profile within the RPB packing.
- Milestone 3.4: The detailed design of the 100 t-CO_2/day RPB and an initial design review is complete. The cost estimation will be completed in the next quarter.
- Milestone 5.1: Discussions with multiple potential host sites have been started and will be continued in the coming quarters.
- Milestone 6.2: Discussions with multiple stakeholders across the value chain were completed in the first quarter. A stakeholder map was outlined and included in an initial T2M Plan. Stakeholder outreach will continue in the coming quarters.

Milestone 3.2 – CFD Modeling

Problem formulation

In FY2024, we developed a CFD model to predict the cooling performance of hot mixed gases within a Direct Contact Cooler (DCC) under various operational conditions, such as the rotational speed of the Rotating Packed Bed (RPB) and the mass flow rates of both liquid and gas. The CFD model uses the same scale and 3D geometry, as shown in Figure 1, as the benchmark experiment, ensuring consistency.

One key advancement is the replacement of the outdated nozzle from Phase 1 with a new design, as shown in Figure 1(a), identical to the one used in current experiments. The liquid enters the DCC through this newly designed nozzle, which features four spreading ports. The cold liquid directly contacts the hot mixed gas—comprising air, CO_2, and H_2O—introduced through the gas inlet. As the gas passes through the porous packing structure, heat transfer occurs between the cold liquid and the hot gas, driving phase transition like evaporation and condensation. This process cools the hot gas and reduces the water vapor fraction within the gas mixture.

The cooling performance is closely tied to the RPB's rotating speed, which affects the dynamic flow within the DCC, as well as the mass flow rates of the liquid and gas upon entering the DCC. To accurately simulate these physical phenomena and capture the effects of different operational conditions, we developed an integrated CFD model that accounts for dynamic flow, heat transfer, mass transport, and phase transition throughout the cooling process.

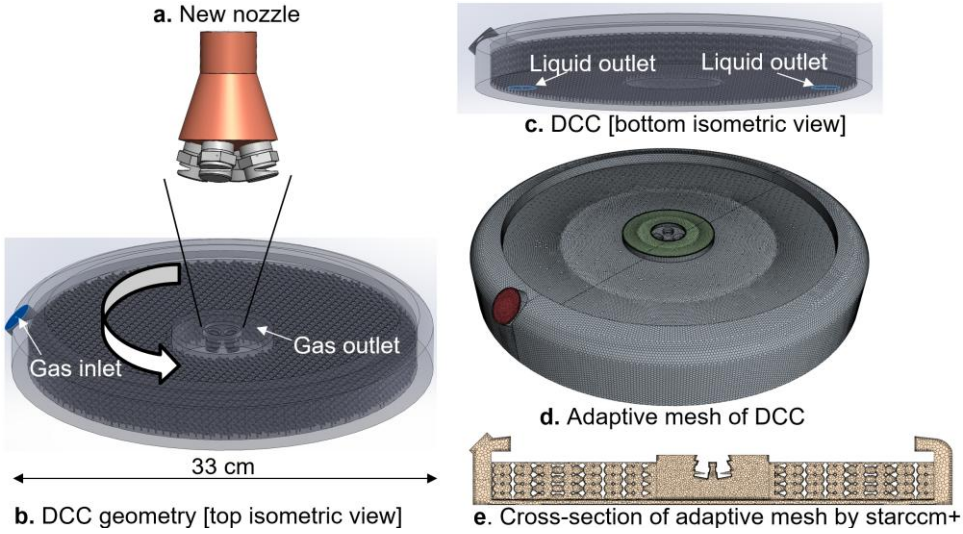

Figure 1 Geometry of DCC employed in CFD modeling. (a) Latest nozzle design featuring four spreading ports for liquid distribution; (b) Top isometric view of DCC with a benchmarking size of 33 cm, showing the gas inlet and outlet and RPB rotating direction; (c) Bottom isometric view of DCC, showing the liquid outlet positioned at the bottom surface. (d) Adaptive mesh of DCC geometry in STAR-CCM+ simulation. (e) Cross-sectional view of the adaptive mesh at the plane indicated in (d).

Mathematical model

To effectively capture the complex physics involved in the DCC process, we have developed an integrated CFD model that combines multiple governing equations. These equations describe the dynamics of fluid flow, mass transport, phase transitions, heat transfer, and liquid-gas interface evolution.

Navier-Stokes Equation (Flow Dynamics)

The N-S equations govern the motion of fluid substances and are fundamental to fluid dynamics. The equation can be expressed as

$$\frac{\partial(\rho \boldsymbol{u})}{\partial t} + \nabla \cdot (\rho \boldsymbol{u}\boldsymbol{u}) = -\nabla P + \nabla \cdot [\mu(\nabla \boldsymbol{u} + \nabla \boldsymbol{u}^T)] - \nabla \cdot \boldsymbol{\tau} + \rho \boldsymbol{g} - \boldsymbol{F}_{st}$$

where ρ is the density, t is the time, $\boldsymbol{u}$ is the velocity field, P is the pressure, μ is the dynamic viscosity, $\boldsymbol{\tau}$ is the Reynolds stress tensor representing the turbulent momentum transport, $\boldsymbol{g}$ represents gravitational acceleration, $\boldsymbol{F}_{st}$ is the surface tension force acting on the liquid/gas interface.

The left-hand side of the Navier-Stokes equation represents the change in momentum due to fluid motion, while the right-hand side accounts for driving forces, including pressure gradients, viscous forces, gravitational forces, and surface tension.

The volume of Fluid model (multi-phase evolution)

The VOF model is crucial for tracking the interface between the liquid and gas phases and is described by:

$$\frac{\partial \alpha_L}{\partial t} + \nabla \cdot (\alpha_L \boldsymbol{u}) = \frac{S_L}{\rho_L \alpha_L}$$

where α_L denotes the volume fraction of liquid phase, *and* S_L is the mass source term due to condensation. In the multi-phase system, $\alpha_L = 0$ represents a pure gas cell, $\alpha_L = 1$ means a pure liquid cell, and $0 < \alpha_L < 1$ means a liquid-gas mixed cell with a volume fraction of gas being $1 - \alpha_L$. The effective properties of the material at a cell are computed based on the local volume fractions of each phase:

$$\rho = \alpha_L \rho_L + (1 - \alpha_L)\rho_g, \quad \mu = \alpha_L \mu_L + (1 - \alpha_L)\mu_g$$

The subscripts L and G represent the pure phase of liquid and gas, respectively.

Surface Tension Force

The surface tension force, $\boldsymbol{F}_{st}$ in the N-S equation, acting on interfacial cells ($0 < \alpha_L < 1$) is determined based on the local interface curvature κ and gradient of liquid volume fraction $\nabla \alpha_L$:

$$\mathbf{F}_{st} = \frac{\sigma_{st} \rho \kappa \nabla \alpha_L}{2(\rho_L + \rho_G)}$$

Here, σ_{st} is a surface tension coefficient, a material property of the two phases in contact. Basically, at room temperature, the surface tension of water is approximately 72.8 nN/m, which is employed in CFD modeling. The surface tension is essential for accurately capturing the behavior of the interface between the liquid and gas phases, influencing the flow dynamics and phase interactions during the cooling process.

Phase Transition Model (Condensation and Evaporation)

In the VOF model, the mass source term S_L, representing the rate of phase change in condensation, is calculated by Lee's phase change model:

$$S_L = \begin{cases} r_{cond}\alpha_{wv}\rho_{wv}\dfrac{T - T_{sat}}{T_{sat}}, & if\ T < T_{sat}, condensation \\ r_{ev}\alpha_L\rho_L\dfrac{T_{sat} - T}{T_{sat}}, & if\ T \geq T_{sat}, evaporation \end{cases}$$

Here, r_{cond} and r_{ev} are the mass transfer rate coefficients for condensation and evaporation processes, respectively. $\alpha_{wv}\ and\ \rho_{wv}$ are volume fraction and density of water vapor, respectively. T_{sat} is the saturation temperature (set as $40°C$ for this model).

The phase change model indicates that condensation occurs when the temperature T is lower than the saturation temperature T_{sat}, while evaporation takes place when T exceeds T_{sat}.

Heat Equation (Heat Transfer)

The temperature T is updated by solving the heat equation, which accounts for heat convection, heat conduction, and the source term due to phase transitions:

$$\frac{\partial T}{\partial t} + \nabla \cdot (\boldsymbol{u}T) = \nabla \cdot (k\nabla T) + \frac{S_E}{\rho C_v}$$

Here, k is the thermal conductivity of the liquid, C_v is the specific heat capacity at constant volume. S_E is the source term of heat, calculated as $S_E = h_{LG}S_L$, with $h_{LG} = 2260\ kJ/kg$ is the latent heat of water vapor condensation. This heat equation renews the temperature field throughout the DCC domain, incorporating the effects of fluid flow, phase transitions, and heat generation from condensation.

Mass Transport of Multi-Species Mixed Gas

In the phase change model, we need to know the volume fraction α_{wv} of water vapor in the mixed gas of water vapor, CO2, and air. The mass transport of multi-species mixed gas is calculated by the diffusion-convection-reaction equation:

$$\frac{\partial c_i}{\partial t} + \nabla \cdot (\boldsymbol{u}c_i) = \nabla \cdot (D_i\nabla c_i) + W_i$$

where c_i is the concentration of species i, D_i is the diffusivity coefficient of the species i, and W_i is the sink term of water vapor due to condensation. $W_i = -\frac{S_L}{(1-\alpha_L)\rho_G}c_i$ for $i = H_2O$ at interface; otherwise, $W_i = 0$.

In summary, for the first time, the integrated model simulates the multi-physics in DCC .The Volume of Fluid (VOF) model tracks the interface and spatial composition of the multi-phase system under the influence of dynamic flow and phase transitions. The Navier-Stokes (NS) equation governs the dynamic flow of both liquid and gas phases. The phase transition model captures the condensation of hot water vapor as it contacts cooler liquid water, accounting for phase transitions in response to flow and temperature conditions. The heat transfer model computes the temperature distribution across the DCC domain, influenced by flow and phase transition effects. The mass transport model describes the diffusion and convection of species such as H_2O, CO_2, and air within the gas phase. Together, these physical models are tightly integrated, exchanging data and interfacing with each other to accurately describe the heat and mass transfer, phase transitions, and dynamic flow present in the DCC process.

Model configurations

In the CFD model, boundary conditions are crucial for defining operational parameters. We assumed all solid walls to be adiabatic and non-slip, meaning there is no heat transfer or media movement through the

walls. All solid boundaries remain stationary except for the Rotating Packed Bed (RPB), which rotates around its central axis. The rotational speed of the RPB can be explicitly defined within STAR-CCM+.

At the liquid inlet of the nozzle, the temperature and flow rate of the liquid are fixed and remain constant over time. Similarly, the temperature, flow rate, and gas composition are also kept constant for the gas inlet. The gas composition at the inlet consists of 88.7% air, 4.5% CO2, and 6.8% H2O by volume, as employed in experiments.

For the simulation, we utilized STAR-CCM+'s built-in material properties library, keeping all default material properties. Adaptive meshing was employed to optimize computational efficiency while maintaining desirable accuracy. In regions of high velocity and near walls, fine mesh was applied to capture turbulent flow and the no-slip condition accurately. In contrast, coarse mesh was used in low-velocity regions and areas far from the solid walls to improve efficiency. To minimize computational load, we implemented an adaptive time-stepping algorithm, a feature of STAR-CCM+ version 23, allowing the time step to adjust dynamically based on the solution requirements, balancing efficiency and accuracy.

Results

Showcase of CFD modeling results.

By solving the integrated CFD model with the specified configurations, the STAR-CCM+ simulation reproduces the critical dynamic processes of liquid movement, gas transport, and temperature distribution across the DCC domain, as illustrated in *Figure 2*. The simulation also enables real-time monitoring of key parameters, such as the temperature of the outflowing liquid and gas, the composition of the outflowing mixed gas, the pressure drop of the gas, and the interfacial area between the liquid and gas within the RPB, as shown in *Figure 3*.

These outputs allow us to evaluate the reliability of the CFD model by comparing it to experimental data. Furthermore, they enable us to investigate the effects of various operational conditions on the cooling performance within the DCC, helping to optimize the system's design and operation.

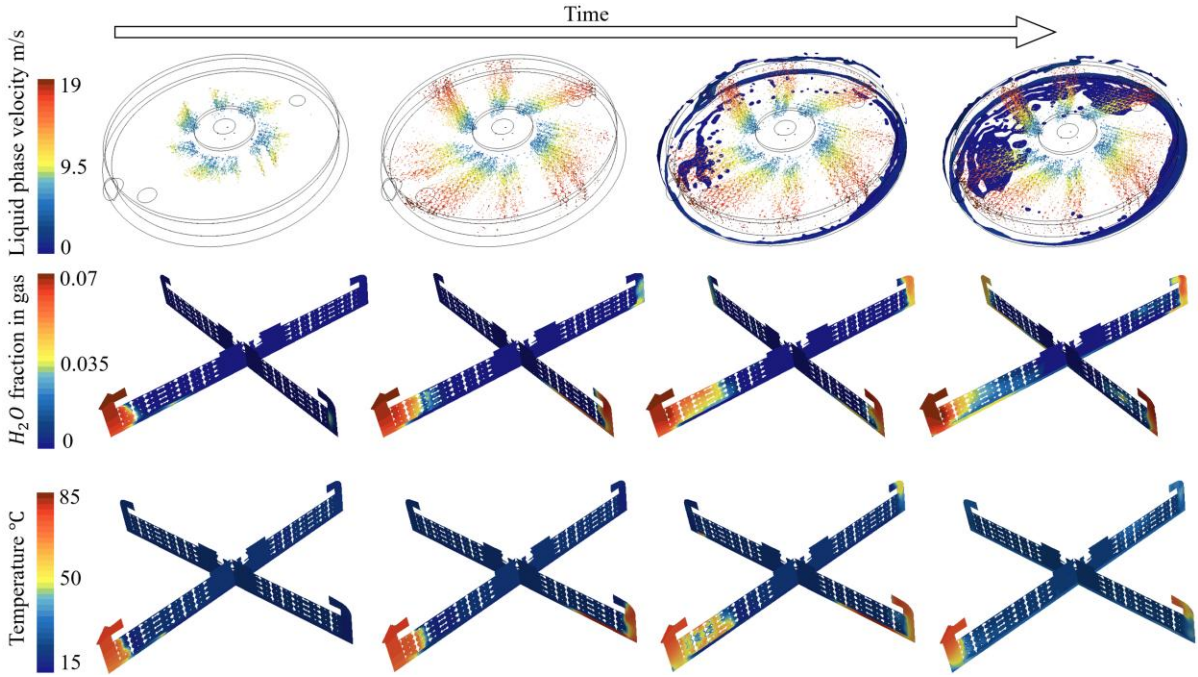

Figure 2 Screenshots of liquid phase velocity, H_2O fraction, and temperature distribution at selected time points, obtained from CFD modeling under the operational condition defined by case 1 in Table 1.

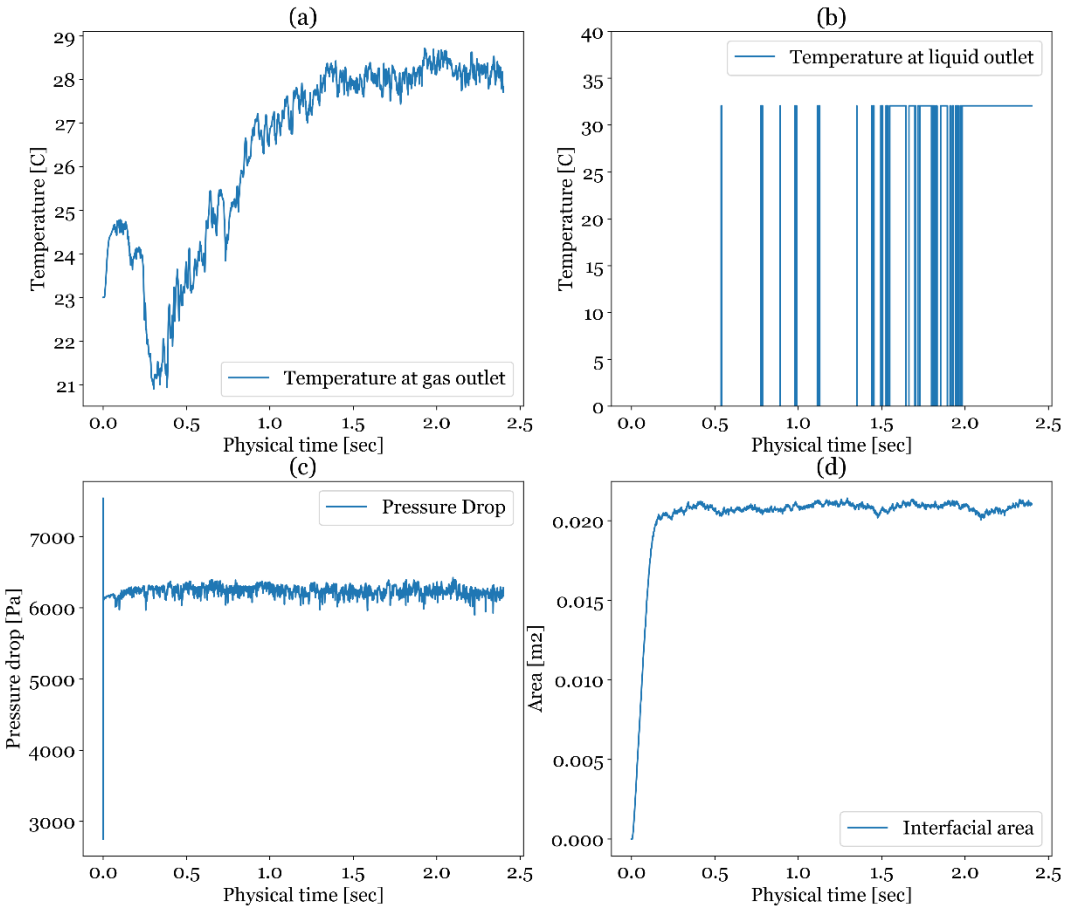

Figure 3 Real-time monitoring of temperature of gas and liquid at outlets, pressure drop, and interfacial area, obtained from CFD modeling under the operational condition defined by case 1 in Table 1.

Table 1 Experimental data of DCC cooling outcomes under various operational conditions.

	Operational conditions						**Outcomes**	
Case #	Gas flow rate (SLPM)	Gas temp at inlet (°C)	Liquid flow rate (kg/min)	Liquid temp at inlet (°C)	L/G ratio	RPB speed (rpm)	Gas temp at outlet (°C)	Liquid temp at outlet (°C)
1	266.1	84.0	1.38	20.7	4	300	29.3	31.4
2	266.1	85.0	1.38	22.3	4	1200	30.6	28.3
3	354.8	84.7	1.84	26.2	4	1200	29.5	34.1
4	177.4	84.9	0.92	23.4	4	1200	41.7	32.8

To evaluate the accuracy of the developed integrated CFD model, we conducted simulations using STAR-CCM+ with identical configurations and operational conditions as experiments listed in *Table 1*. Cases 1 and 2 employ identical configurations, differing only in the rotational speed of the RPB, allowing for an

analysis of the impact of RPB speed on cooling performance. Cases 2, 3, and 4 also share identical configurations but vary the mass flow rates of the liquid and gas. Importantly, the mass ratio of liquid to gas remains constant in these cases; thus, as the mass flow rate of gas increases, the liquid flow rate increases proportionately. This setup enables the assessment of how varying mass flow rates influence cooling performance.

The CFD results for the temperatures of the outflowing liquid and gas under the four operational conditions are directly compared with experimental data, as shown in *Figure 5*. The parity plot illustrates that the data points for both liquid and gas phases are closely aligned with the line $y = x$, indicating that the CFD predictions correspond well with the experimental measurements. This close alignment validates the effectiveness of the developed integrated CFD model in accurately predicting the cooling performance of the DCC under the specified operational conditions.

Effect of RPB rotating speed. To evaluate the effect of the Rotating speed on the cooling performance within the DCC, we compared the data for cases 1 and 2 (*Figure 5*). The simulation results show a clear trend: as the RPB rotating speed increases, the liquid's heat absorption capacity decreases (blue dots in *Figure 5*). This can be attributed to the shorter contact time between the liquid and gas at higher rotational speeds, which limits the amount of heat the liquid can absorb during the cooling process. However, the gas cooling remains relatively unaffected by the rotational speed (*Figure 5*, red dots). The gas flow is less sensitive to rotation, resulting in minimal variation in gas temperature across different rotational speeds.

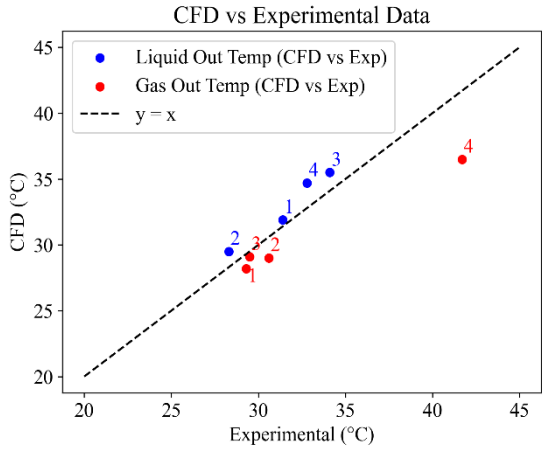

Figure 5 Comparison of CFD results and experimental data on the temperature of outflowing liquid (blue dots) and gas (red dots).

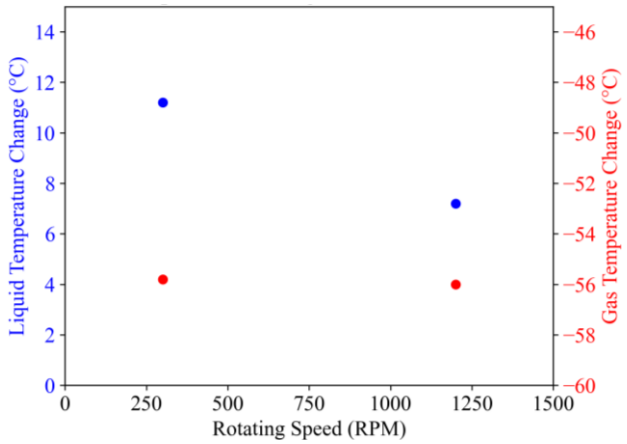

Figure 5 Temperature of outflowing liquid (blue dots with left axis) and gas (red dots with right axis) under different RPB rotating speeds, represented by cases 1 and 2 in

.

Effect of mass flow rate. The effect of mass flow rate on cooling performance was investigated by comparing cases 2, 3, and 4, where the liquid-to-gas (L/G) ratio was held constant (*Figure 7*). For the liquid phase, the results show no clear monotonic relationship between mass flow rate and outlet temperature (*Figure 7*, blue line). The reason is that, at higher mass flow rates, the liquid experiences a shorter contact time with the gas, which limits heat absorption. However, the larger liquid mass flow rate also increases the liquid-gas interfacial area (*Figure 7*), enhancing heat transfer and somewhat offsetting the reduced contact time. These competing effects result in no consistent trend in the liquid temperature at the outlet. For the gas phase, a distinct pattern is observed: at lower mass flow rates, the gas cooling = is less efficient (*Figure 7*, red line). This is because low flow rates significantly reduce the liquid-gas interfacial area, limiting the amount of heat that can be transferred from the gas to the liquid. Therefore, increasing the

interfacial area through higher mass flow rates leads to better cooling performance, particularly for the gas phase.

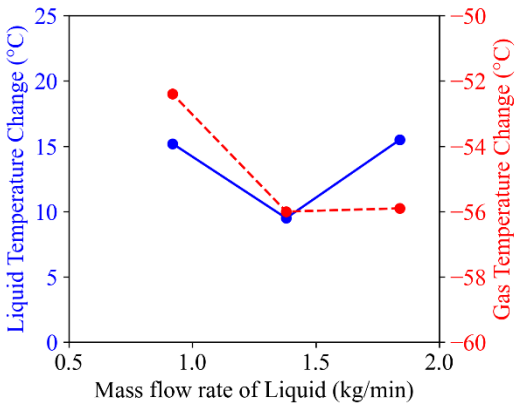

Figure 7 Temperature of outflowing liquid (blue dots with left axis) and gas (red dots with right axis) under different mass flow rates, under cases 2-4 in Table 1.

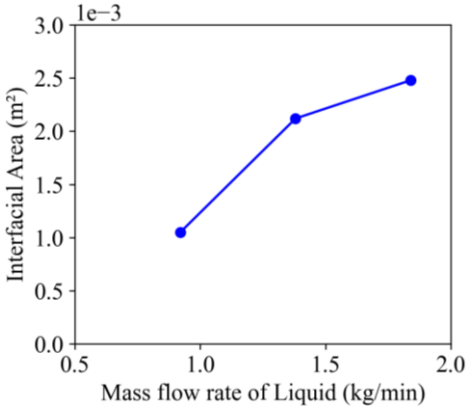

Figure 7 Interfacial areas under different mass flow rates, obtained from CFD modeling under cases 2-4 in

.

In summary, the results suggest that RPB rotating speed mainly affects the liquid phase, with faster speed reducing liquid heat absorption due to shorter contact times. Gas cooling is less sensitive to changes in RPB rotating speed. Liquid mass flow rate has a complex effect on the liquid phase, where higher rates can both decrease contact time, reduce heat absorption, and increase interfacial area, enhancing heat transfer. For the gas phase, a higher liquid mass flow rate improves cooling by increasing the liquid-gas interface.

Future plan

We will develop a scale-up RPB absorber model aimed at predicting CO2 capturing performance of large-scale RPBs. To manage the computational demands associated with simulating large-scale RPB systems, we will simplify the packed structure by treating it as an equivalent porous medium.. This approach will significantly reduce the computational load compared to modeling the exact 3D geometry of the porous packing. Once this absorber model is validated against experimental data, it will enable us to explore the effects of RPB scale-up on CO2 capturing efficiency. The ability to simulate different scales of the RPB absorber will provide valuable insights into the optimization of design and operational parameters, ultimately leading to enhanced performance in CO2 capture.

Pacific Northwest National Laboratory

902 Battelle Boulevard
P.O. Box 999
Richland, WA 99354

1-888-375-PNNL (7665)

www.pnnl.gov